

Homebuilt single-molecule scanning confocal fluorescence microscope studies of single DNA/protein interactions

Haocheng Zheng^a, Lori S. Goldner^b, Sanford H. Leuba^{a,*}

^a *Department of Cell Biology and Physiology, University of Pittsburgh School of Medicine, Department of Bioengineering, School of Engineering, University of Pittsburgh Cancer Institute, Hillman Cancer Center, 5117 Centre Avenue, Pittsburgh, PA 15213, USA*

^b *Physics Laboratory, National Institute of Standards and Technology, 100 Bureau Drive, Gaithersburg, MD 20899, USA*

Accepted 14 November 2006

Abstract

Many technical improvements in fluorescence microscopy over the years have focused on decreasing background and increasing the signal to noise ratio (SNR). The scanning confocal fluorescence microscope (SCFM) represented a major improvement in these efforts. The SCFM acquires signal from a thin layer of a thick sample, rejecting light whose origin is not in the focal plane thereby dramatically decreasing the background signal. A second major innovation was the advent of high quantum-yield, low noise, single-photon counting detectors. The superior background rejection of SCFM combined with low-noise, high-yield detectors makes it possible to detect the fluorescence from single-dye molecules. By labeling a DNA molecule or a DNA/protein complex with a donor/acceptor dye pair, fluorescence resonance energy transfer (FRET) can be used to track conformational changes in the molecule/complex itself, on a single molecule/complex basis. In this methods paper, we describe the core concepts of SCFM in the context of a study that uses FRET to reveal conformational fluctuations in individual Holliday junction DNA molecules and nucleosomal particles. We also discuss data processing methods for SCFM.

© 2007 Elsevier Inc. All rights reserved.

Keywords: Scanning confocal fluorescence microscope; Nucleosome; Holliday junction; Four-way junction DNA; Single-molecule dynamics; Single-pair fluorescence resonance energy transfer

1. Introduction

Bulk assays that have traditionally been used to study nucleosome dynamics have been very successful at determining overall nucleosomal movements on DNA. These same assays are, however, limited in their ability to elucidate fast reversible processes that cannot be easily synchronized, or to investigate differences between individual molecular complexes. Recent improvements in instrumentation have made possible a single-molecule approach to biology, in which one macromolecule is studied at a time (reviews can be found in Refs. [1–6]). Using single-molecule techniques, it is possible to study both the details of a

molecular ensemble as well as the kinetics of individual members of the ensemble.

Single-molecule approaches have already led to significant new information about chromatin dynamics, reviewed in [7–17]. Examples are the determination of the piconewton (pN)¹ forces to unravel individual nucleosomes [18–24], the demonstration that stretching forces applied to DNA prevent nucleosome assembly [18,25–27], and the observation of reversible long-range opening and closing in indi-

¹ *Abbreviations used:* 4WJ, four-way junction; APD, avalanche photodiode; FRET, fluorescence resonance energy transfer; E_{app} , apparent efficiency of FRET; E_{FRET} , efficiency of FRET; EFM, evanescent field fluorescence microscopy; fl, femtoliter; I/O, input/output; NA, numerical aperture; pN, piconewton; p/n structure, positive/negative structure; ms, millisecond; nm, nanometer; SCFM, scanning confocal fluorescence microscope; SNR, signal to noise ratio; spFRET, single-pair fluorescence resonance energy transfer; TTL, transistor–transistor–logic.

* Corresponding author. Fax: +1 412 623 4840.
E-mail address: leuba@pitt.edu (S.H. Leuba).

vidual nucleosomes in real time [28]. Single-molecule approaches can be used to achieve a fundamental understanding of biological processes occurring at the nanometer (nm) scale, in the millisecond (ms) time domain and at the pN force level.

A scanning confocal fluorescence microscope (SCFM) that is sensitive enough to detect single-fluorescent molecules can be used to observe single-pair fluorescence resonance energy transfer (spFRET) [29–45]. Fluorescence resonance energy transfer (FRET) is a spectroscopic process in which non-radiative energy transfer occurs between an excited dipole (the donor) and another dipole (the acceptor) that has an absorption spectrum that overlaps the emission spectrum of the donor [46]. The probability of energy transfer, also called the FRET efficiency (E_{FRET}), is dependent on the distance between two dipoles, R , and can be expressed as $E_{\text{FRET}} = [1 + (R/R_0)^6]^{-1}$ where R is the distance between two dipoles. The Förster distance, R_0 , can be calculated from the spectral properties of donor and acceptor and their relative orientation [46–48]. A typical value of R_0 for freely rotating dyes is 5 nm, and so E_{FRET} is a sensitive measure of R over an approximate range of 1–10 nm. In much of the FRET literature, the angular dependence of R_0 is ignored and the dyes are assumed to freely rotate, so that measuring E_{FRET} permits R to be determined: hence the frequent name “spectroscopic ruler” for FRET [47].

Single molecular-pair FRET has been previously reviewed by Ha [49]. In a typical experiment involving spFRET, a donor dye and an acceptor dye are covalently attached to known sites within a macromolecule. The macromolecule is tethered to a surface to prevent it from diffusing out of the detection volume of the SCFM. Changes in the conformation of the molecule are detected as changes in the energy transfer between the donor and acceptor molecule. In this fashion, single molecular-pair FRET has been used to study, e.g., nanometer conformational motions in individual RNA molecules [29–35], individual DNA molecules [36–41] and individual helicases and other motor proteins on DNA [42–45]. By following changes in FRET efficiency over time, it is possible to observe nanometer distance changes due to macromolecular rearrangements. In this way, FRET can be used to investigate a variety of biological phenomena that produce changes in molecular proximity (Fig. 1).

It has also been possible to use confocal microscopy and spFRET to study single-nucleic acid or protein molecules in solution [50–58]. In this case, the molecule is observed only during its transit time across the detection volume of the microscope. To increase the detection time but avoid the need to immobilize molecules on a surface, researchers have used tethered lipid vesicles to contain the molecule under study in the detection volume [59–61]. Most recently spFRET has been demonstrated on molecules confined to a water droplet optically trapped in the detection volume [62].

Fluorescence from single fluorophores does not require a confocal microscope to observe and several other modalities

for decreasing background have been successful. These include e.g., a modified version of flow cytometry [63,64] used for single-fluorophore detection and near-field microscopy [65–67], evanescent-field fluorescence microscopy (EFFM, also called total internal reflection microscopy [68]) [69], and versions of epi-fluorescence microscopy [70–73] used for single-fluorophore imaging. In the case of low temperature experiments, reviewed in Ref. [1], inhomogeneous broadening makes background reduction possible through spectral selection, so some of the earliest single-stationary fluorophore experiments were done at low temperatures [74–77].

The adaptation of confocal microscopy [78] first to detect [79,80] and then to image [81,82] single fluorophores at room temperature made the technique widely available. The first demonstration of spFRET from immobilized molecules at room temperature was performed using a near-field microscope [83]. Since then, many groups have applied spFRET to study biomolecules and biomolecular complexes using microscopies (such as confocal or EFFM) that are easily adapted to an aqueous environment.

Many groups have contributed to the state-of-the-art in single-molecule fluorescence and reviews have been written on the topic of spFRET [49,84], single-molecule optical techniques in general [1,3,5,6,85–89], and their application to biological systems [2–4,87,90–95]. In this paper, we restrict ourselves to a review of confocal microscopy and spFRET used to study DNA/protein interactions.

Confocal imaging greatly improved background rejection in optical microscopy by minimizing the illuminated volume and simultaneously excluding out-of-focus light from the detector. Combined with highly efficient photon counting detectors, it is possible to collect enough signal and reject enough background (and its associated noise) to make fast detection of single fluorophores possible. In confocal imaging, the sample is illuminated by focusing a laser beam into a diffraction limited volume with a high numerical aperture (NA) objective, and the fluorescence light collection is typically done through the same objective (epi-fluorescence set-up). The fluorescence collected from the focal volume of the laser is imaged onto a pinhole, the size of which is chosen to maximize throughput from the illuminated region while rejecting out-of-focus scattered light. The combination of focused excitation laser and collection pinhole gives a detection volume that is approximately 1 fl.

To make images of molecules that are immobilized on a surface, the sample or focused laser has to be scanned in the x - and y -dimensions. Alignment of the focal volume and pinhole is critical and so sample scanning, rather than laser scanning, is often employed to form an image in a typical home-built apparatus to avoid the complications of maintaining alignment and throughput while scanning the laser.

Commercial instruments capable of single-molecule imaging are now widely available but prohibitively expensive for many laboratories. Here we describe a simple and inexpensive instrument suitable for single-molecule studies that can be built on a much smaller budget.

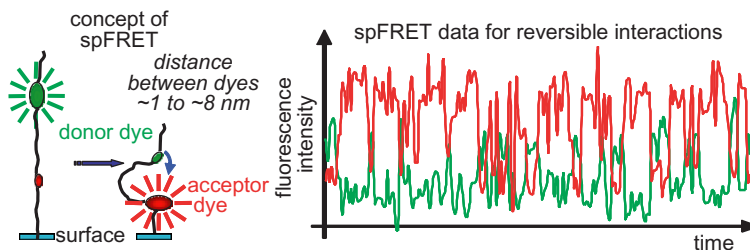


Fig. 1. Concept of single pair fluorescence resonance energy transfer (spFRET) and example time trajectory. FRET [105] occurs if the distance between the two dyes is between 0 and about 10 nm. The value of FRET is dependent upon the proximity and relative orientation of the two dyes within this range [48]. In many cases, the dipole moments of the acceptor and donor dye are able to rotate in all directions so that the orientation effects are averaged [49]. Polarization anisotropy measurements can be used to determine the degree to which the dyes are freely rotating. So long as changes in FRET can be linked to a biochemical event [49] it may not matter whether the change in FRET is due to a change in polarization and/or a change in distance. In FRET, the probability of energy transfer is 50% at R_0 , a characteristic distance for each dye pair. The R_0 is 6 nm for cyanine Cy3/Cy5 donor/acceptor pair [33]. If the molecule undergoes reversible conformational transitions, the intensities of the two dyes will change in an anticorrelated manner with time. Most spFRET studies use relative changes in the FRET signal to follow dynamics rather than absolute distance changes [49].

2. Instrumentation

The scheme of the SCFM set-up is depicted in Fig. 2, and photographs of the system are shown in Fig. 3. Light from an excitation laser passes through a beam expander that increases the diameter of the laser beam so that it fills the back aperture of the objective. The laser is then reflected by a dichroic mirror into the high NA microscope objective. The backscattered fluorescence from the specimen is collected by the same objective, passes through the dichroic mirror and is focused onto the single-photon sensitive APD detectors. Sample scanning is performed by an x - y -piezo stage. The active region of the APD has a diameter of 175 μm and so it acts as its own pinhole.

A single-molecule sensitive SCFM system requires high mechanical stability, a sufficiently stable laser source with a beam of constant intensity and profile, and a photoelectron detector with data acquisition electronics for the timescale of the sample under study. The major challenge is synchronizing data collection with scanning and aligning the optics.

The following subsections give step-by-step descriptions of the parts of a complete SCFM set-up.

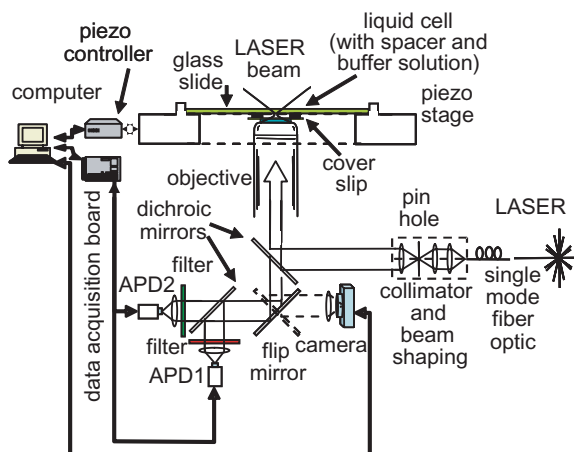


Fig. 2. Schematic of scanning confocal fluorescence microscope (SCFM).

2.1. Excitation laser sources

To achieve diffraction limited focusing, the excitation laser source should have a good Gaussian intensity profile. Excitation wavelengths need to be chosen to match the

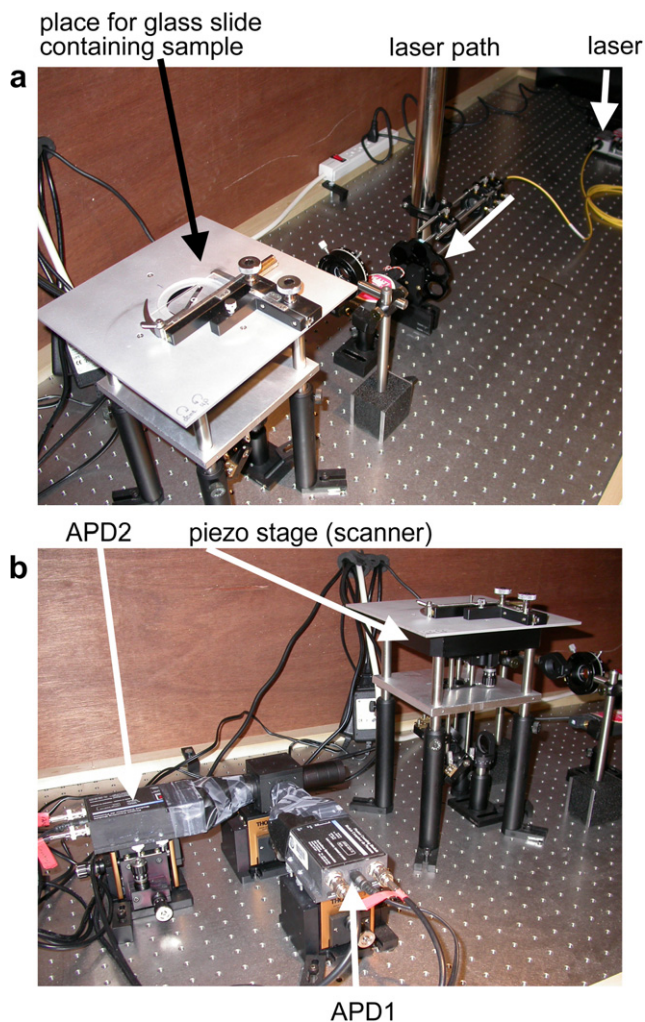


Fig. 3. SCFM using avalanche photodiodes (APDs). (a) Photograph of the laser, laser path, mounts for glass slide containing sample and piezo stage (scanner) of the SCFM. (b) Photograph of the APDs portion of the SCFM.

absorption spectra of the fluorophores under study, and the power should be sufficient to saturate the optical transition (a few milliwatts, although this much power will not generally be needed for imaging single molecules). Pointing stability (directional stability of the beam) and power stability also need to be considered.

To excite the donor dye for the FRET experiments, the wavelength of the laser source should be well within the excitation band of the donor dye. In our experiments, Cy3 dye [96] is the donor and we use 532 nm excitation light, provided by a miniature solid-state diode pumped laser module (GM32-5SL) from Intelite Inc. This is a continuous wave laser with a single-longitudinal mode (5 mW maximum power) output coupled to a single-mode fiber. The laser is internally temperature stabilized to minimize drift in the power output.

The flexibility of the design of the SCFM allows for the introduction of lasers of other wavelengths [97–99]; having multiple lasers allows one to design experiments following more than one event as well as having an external check on the photo-stability of the dyes.

2.2. Dichroic mirrors, excitation and emission filters

A typical SCFM used for spFRET has four optical filters to separate the excitation light from the fluorescence and to separate light from the donor and acceptor channels. Interference filters are preferred in SCFM because of their sharp band edges and the high fidelity in their rejection and transmission characteristics. We are using interference filters from Chroma Technology Corp for our setup: (1) a Z532RDC-532 nm dichroic mirror to separate the sample signal from the excitation laser source; (2) a 620DCXR-620 nm dichroic mirror to separate the donor and acceptor signals into two channels; (3) a HQ585-70M band pass filter to filter out the donor signal to one APD detector; and (4) a E645LP long pass filter to filter out the acceptor signal to the other APD detector. The wavelength properties of these dichroic mirrors and filters were chosen for their suitability with Cy3 and Cy5 cyanine dyes [96].

2.3. Microscope objective and tube lens

Because the same objective lens is used for both illumination and light collection of the sample in SCFM, the objective is the most important part for the overall performance of the SCFM. The larger the NA of the objective lens, the more light the objective lens can collect and the better the background rejection will be. A water-immersion objective (NA = 1.2) or an oil-immersion objective (NA = 1.4) is typically used to detect the fluorescence of surface-immobilized molecules.

Our SCFM uses an infinity-corrected objective lens. An infinity lens sets the image distance at infinity so that a tube can be used at any point in the optical path to refocus the image onto the APD detector. The intrinsic advantage of

infinity optical systems is to allow introduction of auxiliary components, such as optical filters and polarizers, into the parallel optical path between the objective and the tube lens with only a minimal effect on the focus and aberration corrections.

2.4. Pinhole

In SCFM, the function of the collection pinhole is to minimize the detection volume in all directions and thus to further decrease the background. In general, the pinhole is chosen to match the microscope optics; the pinhole size is related to the size of the focal spot at the image plane. This insures that a majority of the fluorescence light from the detection volume passes through the collection pinhole while background from outside this region is rejected. The pinhole should therefore have approximately the same diameter as the full width at half maximum of the airy diffraction pattern generated by the tube lens at the pinhole's position. Typically, the optimal pinhole diameter is between 30 and 100 μm . So long as care is taken to check that the glass and buffer have minimal background contribution, the actual pinhole size can be a bit larger (making alignment easier) with only nominal increases in background. Since photon-counting APDs typically have a very small detection area (diameter 175 μm), the use of a pinhole can be dispensed with and alignment correspondingly simplified.

2.5. Avalanche photodiode detector (APD)

The APD is a solid-state photodiode that internally amplifies the photocurrent by an avalanche process. As a result, the APD has both high quantum efficiency and high gain.

In APDs, a large reverse-bias voltage, typically over 100 V, is applied across the active region, a positive/negative (p/n) semiconductor structure that can accept photons to generate light-induced current. This voltage causes the electrons initially generated by the incident photons to accelerate as they move through the APD active region. As these electrons collide with other electrons in the semiconductor material, they cause a fraction of them to become part of the light-induced current, a process known as avalanche multiplication. Avalanche multiplication continues to occur until the electrons move out of the active area of the APD.

We are using SPCM-AQR-15 APDs from Perkin-Elmer Life Science. These APDs are self-contained modules that detect single photons of light from 400 to 1060 nm, a wavelength range that covers the entire emission spectrum of both the donor (Cy3) and acceptor (Cy5) dyes. These APDs have a circular active area with a nominal diameter of 175 μm and a peak quantum efficiency as high as 65% at 630 nm. The module is thermoelectrically cooled and temperature controlled and requires a +5 V power supply. The output consists of

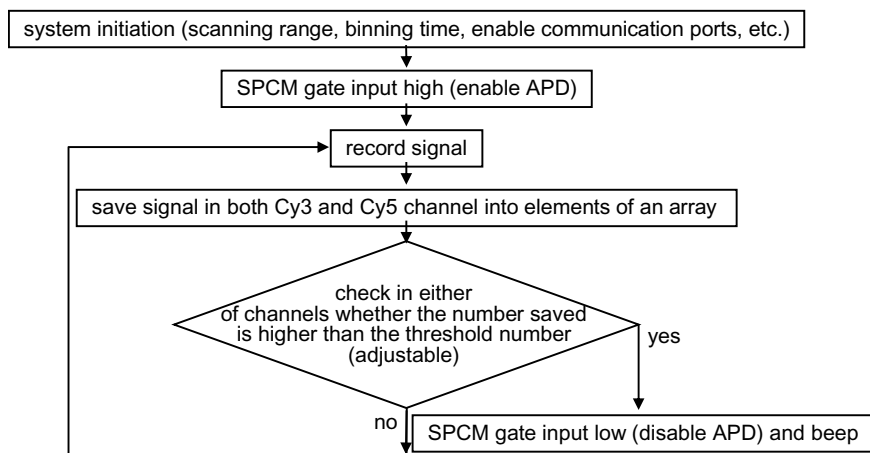


Fig. 4. Flow chart of the algorithm used to protect the APDs from exposure to excess light.

35 ns TTL level pulses with a dead time of 60 ns. Saturation occurs above count rates of 15 MHz.

Excessive light levels can cause the APD chip to over-heat and damage the SPCM module. In our SCFM setup, we pre-set a threshold to limit the light exposure by the APD. If the signal intensity is higher than the preset threshold (APD photon counts greater than the preset threshold number), then the software will automatically shut down the APD. A detailed software flow chart is shown in Fig. 4.

2.6. Data acquisition electronics

A typical electronics device capable of photon counting is the multifunction PC 6602 family card from National Instruments Inc. The 6602 family devices are timing and digital I/O modules for use with computers that have PCI or PXI/CompactPCI slots. They have eight 32-bit counter/timers and up to 32 lines of TTL/CMOS-compatible digital I/O, and we use it for both scanning and data acquisition.

2.7. Scanning piezo-stage

A surface-immobilized single-molecule sample can be scanned to obtain a two-dimensional image. Because the excitation laser beam remains stationary, optical devices can be easily added to the system with small aberration effects. The speed limitations of scanning mechanical parts (piezo-stage and sample holding mounts) are not problematic because scan speed is typically limited by the need to collect photons for at least several milliseconds at each image point. Only slow scan rates are used.

We use a Physik Instruments stage (PI P-527.2CL) that has a scan range of $200\ \mu\text{m} \times 200\ \mu\text{m} \times 50\ \mu\text{m}$. It has a $66\ \text{mm} \times 66\ \text{mm}$ clear aperture, well suited for a SCFM. Low voltage piezoelectric transducers (PZT, 0–100 V) and flexures are employed as the driving and guiding system for stability and repeatability. Integrated capacitive position

feedback sensors provide positioning resolution and stability of a few nanometers in closed loop operation.

2.8. Software for SCFM operation and data analysis

We use software written in Visual Basic from Microsoft to control scanning of the piezo stage to obtain the two-dimensional image of the sample, collect the data from the photon counting board, display and save the time trajectories of fluorescence signals from the donor and acceptor molecules. A detailed flow chart of the operating software is depicted in Fig. 5 and the interface of the operating software is shown in Fig. 6 with a $10\ \mu\text{m} \times 10\ \mu\text{m}$ image of single molecules with a resolution of $0.1\ \mu\text{m}$ per pixel and an integration time of 10 ms/pixel. The arrow depicts a molecule in the image from which both Cy3 and Cy5 fluorescence are emitted. To measure changes in FRET with time, the stage is repositioned so that a molecule identified in such an image is positioned in the confocal detection volume. During the time that photons are collected to generate a FRET trajectory (e.g., Fig. 7a), the confocal volume remains stationary and does not scan. Fluorescent photons are typically counted in 10 ms bins, although it is possible to use bin times of 1 ms or less.

Excel and Origin software are used to calculate the histograms of E_{app} , the apparent efficiency of FRET, and dwell times for the distinguishable conformational states [15]. If we observe two distinct FRET states (e.g., Fig. 7c), then we perform thresholding at 50% between the states.

3. SCFM applications

In the following subsections, experimental results of single-molecule (Holliday junction and mono-nucleosome) fluorescence detection will be reported, demonstrating the capabilities and performance of the SCFM system. A Holliday junction or four-way junction (4WJ) DNA is a model system to represent the portion of the DNA crossover of two sister chromatids [100].

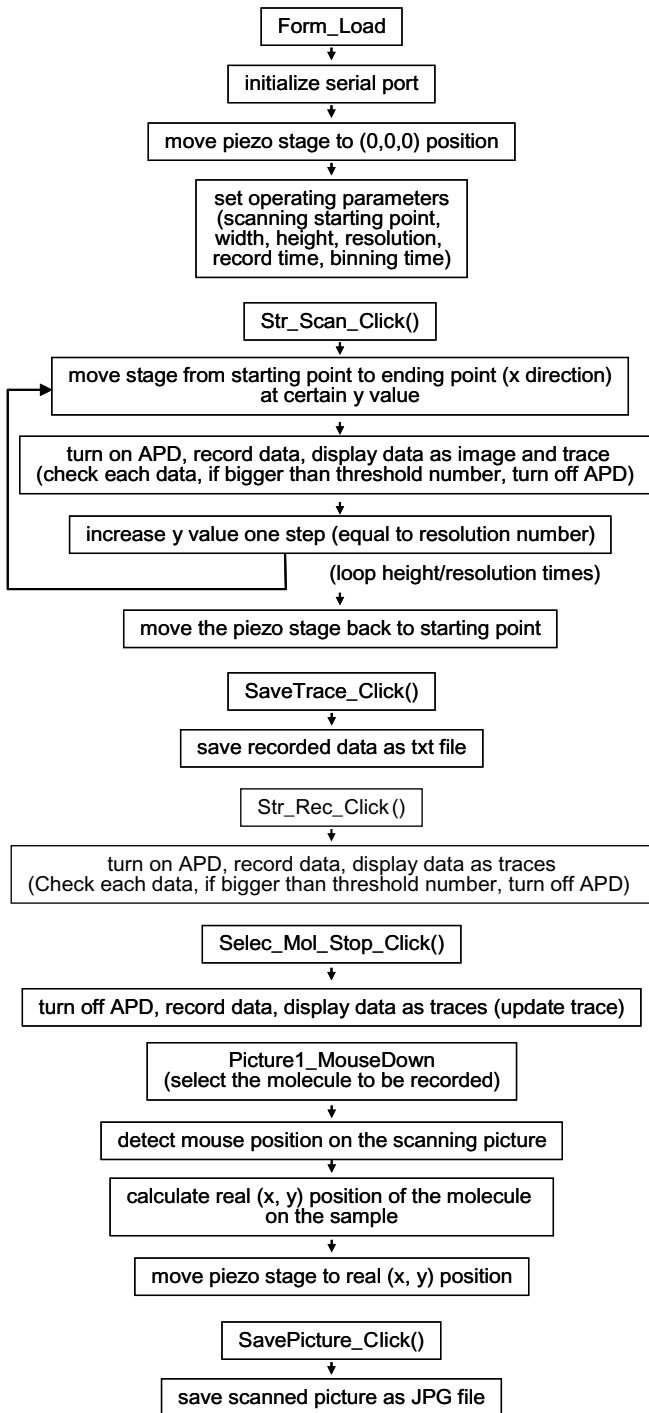


Fig. 5. Detailed flow chart of software operation of SCFM.

3.1. Holliday junction preparation

Oligonucleotides of the following sequences were synthesized using phosphoramidite chemistry implemented on DNA synthesizers (IDTDNA.com): Cy5-J3b, 5'-Cy5-CCTAGCAAGGGGCTGCTACGG; Cy3-J3h, 5'-Cy3-CGTAGCAGCCTGAGCGGTGGG; Biot-J3r, 5'-Biotin-CCCACCGCTCAACTCAACTGGG; and J3x, 5'-CCCA GTT GAGTCCTTGCTAGGG [36]. We mixed all the oli-

gonucleotides together at 65 °C and then allowed them to come slowly to room temperature to hybridize completely.

3.2. Nucleosome preparation

We prepared double-stranded DNA containing both Cy3 and Cy5 cyanine dyes (on opposite strands of the DNA) and a biotin at one end so that the molecule can be attached to a surface via biotin/streptavidin chemistry. Prior to an experiment, the DNA is reconstituted with core histones into a nucleosome, e.g. [13,15,27,28,101].

3.3. Flow cell preparation

We have prepared flow cells as previously described [15].

3.4. Single-molecule measurements

The light from the excitation laser passes through a beam expander to expand the laser beam to fill the back aperture of the objective, and is then reflected by a dichroic mirror (Z532RDC), into a high NA microscope objective. The light emission generated within the specimen is collected by the same objective and focused, after being separated by the dichroic mirror (620DCXR) and emission filters (HQ585-70M for donor and E645LP for acceptor), onto the single-photon sensitive APD detectors. Sample scanning is performed by an x - y piezo stage.

An essential solution additive to slow down the photobleaching of fluorescent dyes is an oxygen scavenger system (e.g., 3% (w/w) glucose, 1% (v/v) β -mercaptoethanol, 0.1 mg/ml glucose oxidase and 0.02 mg/ml catalase) [15,49,102,103]. Recently it has been demonstrated that the addition of Trolox, an analog of vitamin E, with an oxygen scavenger system prevents blinking of Cy5 [104]. As Trolox is an antioxidant, other anti-oxidants may be found useful in preventing Cy5 blinking.

3.5. Data analysis

To analyze the time trajectories of fluorescence signal from a molecule, we first filtered out blinking events (defined as a reversible transition of the acceptor to an inactive state, giving rise to an unquenched donor emission) [29] and photobleaching of either fluorophore, and then performed an analysis on the efficiency of FRET (E_{app}) time traces. E_{app} here is taken to be the measured fluorescence signal from the acceptor divided by the sum of fluorescence signals from both the acceptor and the donor. The crosstalk (laser and fluorescent light leakage through the filters) and background (from dark counts and autofluorescence from the buffer and the glass microscope slide) is subtracted to determine the correct values for the donor and acceptor signal. Background can be measured as the remaining signal after photobleaching of the fluorophores. E_{app} is different from the actual value for the probability of energy transfer because we have not taken into account the difference in

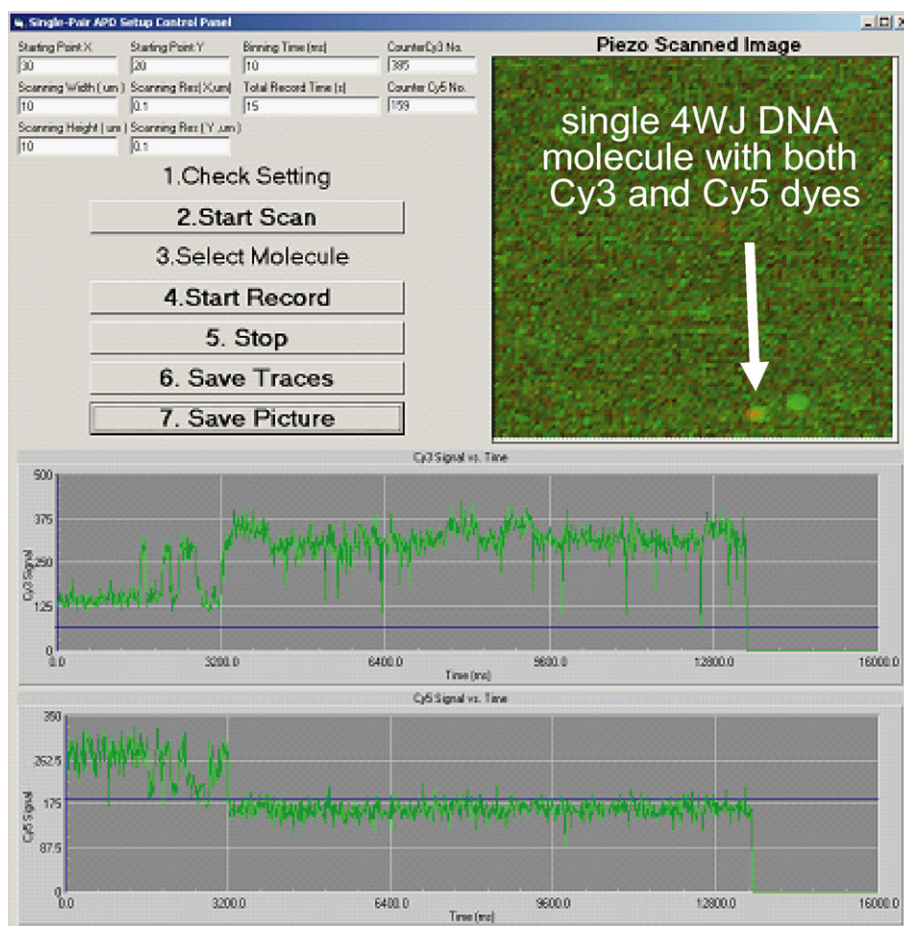


Fig. 6. Video monitor interface of scanning confocal fluorescence microscope operating software containing an image of single molecules ($10\ \mu\text{m} \times 10\ \mu\text{m}$ scan). Arrow points to a single 4WJ DNA molecule in which intensities of both the Cy3 and Cy5 dyes can be observed (pseudo-colored as light green and red, respectively). Positioning this molecule at the confocal detection volume produced the time trajectories of the acceptor and donor channels shown in the bottom portion of the interface. An anti-correlation of the intensities of the donor and acceptor dyes is used to identify the two trajectories as coming from conformational changes occurring in a single molecule.

detection efficiency (E_{FRET}) of the two (donor and acceptor) channels. So long as changes in FRET can be linked to a biochemical event [49] it does not matter that our values for E_{app} are not the same as E_{FRET} .

To calculate the average length of time (τ) that the molecule resides in a specific conformational state, the duration of all events in a high FRET state characteristic of that conformation (or conversely in a low FRET state characteristic of an alternative conformation) from a specified number of molecules were plotted as a histogram and fit to an exponential decay to determine τ . Data analysis results are shown in Fig. 7. This figure demonstrates the dynamics of individual 4WJ DNA molecules that alternate between a high FRET state and a low FRET state. DNA conformations associated with the high FRET and the low FRET state are depicted in the inset to Fig. 7a. When we observed 4WJ DNA molecules with EFFM [15], we found that it was difficult to capture individual DNA molecules in either the high or the low states because the 100 ms camera exposure would average out the signal from both states. Using the SCFM we have found that DNA architectural binding proteins can diminish the difference between the high and low

states as well as change the length of time the DNA molecule resides in either of these two states, which points to new findings on how single-protein molecules can affect dynamics of DNA motions (unpublished observations).

SCFM experiments with nucleosomes are shown in Fig. 8. We have used nucleosome positioning DNA sequences prepared with covalently attached dyes to create FRET when the nucleosome is formed. Using a streptavidin coated surface, the nucleosomes are attached to a microscope glass surface and imaged with the SCFM. Spots in the $10\ \mu\text{m} \times 10\ \mu\text{m}$ scan that have photon counts in both the Cy3 and Cy5 channel are further investigated by placing the confocal volume on each area to generate a time trajectory until photobleaching is observed. From the time trajectory, it is possible to determine E_{app} . The high SNR of the SCFM allows one to easily see the FRET from formed nucleosomes. Biological reactions that unravel nucleosomes should be readily discernable with such single-spectroscopic measurements. We have recently observed long-range conformational changes in individual nucleosomes by spFRET with an EFFM [28]. As the SCFM has a much higher SNR (20:1) than the EFFM ($\approx 5:1$) [49], it

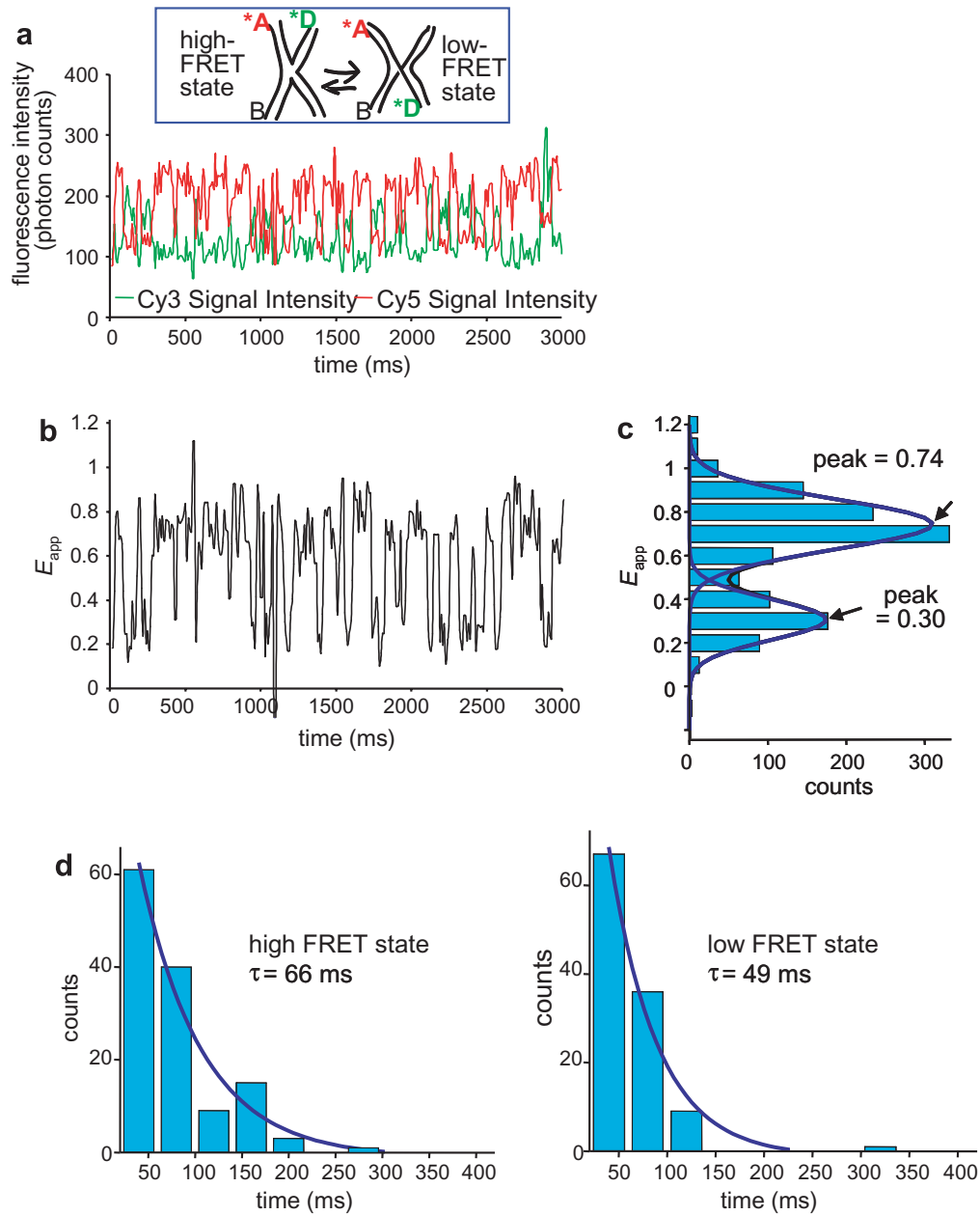


Fig. 7. Time trajectories of spFRET signals and data analysis. (a) Upper traces: time trajectories of Cy3 and Cy5 dyes in a single four-way-junction (4WJ) DNA molecule in 10 mM $MgCl_2$, 50 mM NaCl, 10 mM Tris-HCl, pH 8.0, 3% (w/w) glucose, 1% (v/v) β -mercaptoethanol, 0.1 mg/ml glucose oxidase and 0.02 mg/ml catalase. (Inset) Schematic of dynamic changes of a 4WJ DNA molecule alternating between a high-FRET state, when the donor and acceptor dyes are in close proximity, and a low-FRET state when the two dyes are much further apart. (b) E_{app} analysis of the data in (a). (c) E_{app} distribution of 4WJ DNA of the data in (b). (d) Histograms of dwell times of 4WJ DNA in high-FRET state and low-FRET state of the data in (b). Our 4WJ DNA spFRET data are similar to that obtained by McKinney and coworkers [36].

should be possible to achieve much higher resolution time trajectories with the SCFM, especially if the instrument is connected to a high precision flow injection system, e.g. [13]. With such a flow system, it should be possible to add factors in the middle of a time trajectory to follow what occurs before binding and after binding of the same DNA molecule. It has been recently shown via optical tweezers experiments that there is a small yet significant change in individual nucleosome stability in a chromatin fiber context upon histone acetylation [20]. The high SNR and time reso-

lution of the SCFM should be amendable to following the change in dynamics in individual nucleosomes induced by histone modifications or histone variant substitution.

4. Future directions

In addition to following the dynamics of individual nucleosomes or individual Holliday junctions, the SCFM can be used to follow the actions of motor proteins that act on nucleic acids and nucleosomes such as DNA and RNA

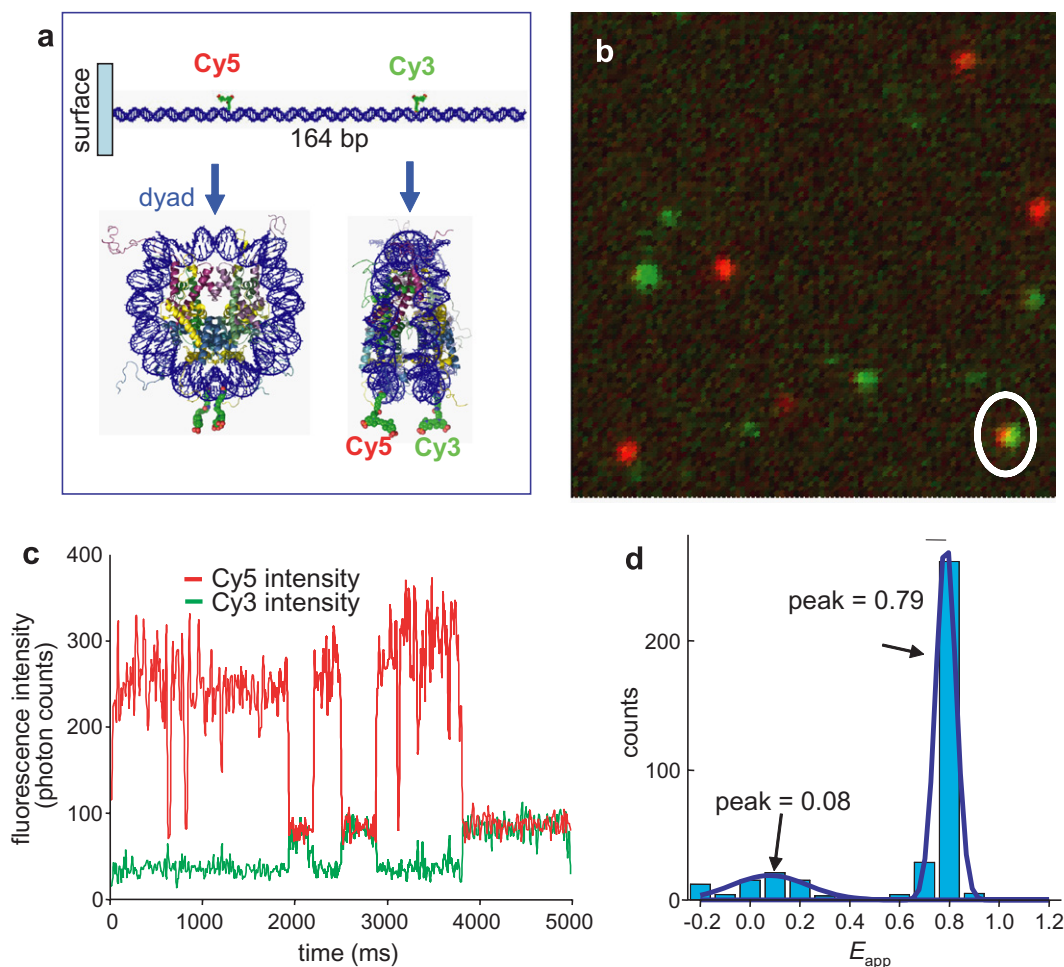


Fig. 8. Nucleosome for SCFM spFRET experiments. (a) Schematic of a nucleosome labeled with a Cy5 and a Cy3 fluorescent dye pair for spFRET apart (top panel). A DNA molecule is prepared with the two dyes 75 bp (≈ 25 nm) apart. Upon reconstitution into a nucleosome (bottom panel), the carbon molecules upon which the dyes are attached should be ≈ 3 nm apart, a distance in which FRET will occur. Left is face view of nucleosome and right is side view of nucleosome with the two dyes. Arrows point to the dyad axis of the nucleosome. Figure, courtesy of Dr. J. Harp, was prepared with PyMOL [106] and Xfit [107] using pdb 1kx5 [108]. For details of preparation see [28]. (b) Example SCFM $10 \mu\text{m} \times 10 \mu\text{m}$ image of individual nucleosomes labeled with a Cy3 dye and a Cy5 dye (for details on labeling see [15,28]). Individual green spots are examples of single Cy3 dye molecules and individual red spots are examples of single Cy5 dye molecules. Spot with both green and red (circled) represents a doubly labeled nucleosome, that can be positioned at the confocal detection volume for further study. (c) SCFM time trajectory of an individual nucleosome in 10 mM Tris–HCl, pH 7.5, 0.5 mM EDTA, 0.4% (w/w) glucose, 1% (v/v) β -mercaptoethanol, 0.1 mg/ml glucose oxidase and 0.02 mg/ml catalase. Each time point is 10 ms of binning. Upper red trace and lower green trace represent the number of photon counts for the Cy5 acceptor dye and Cy3 donor dye, respectively, in a single nucleosome. (d) Histogram of apparent efficiency of FRET.

polymerases, DNA repair and recombination factors, chromatin remodeling factors, etc. We know of no other method other than spFRET with which one can follow the dynamics of reversible processes of single molecules in real time, e.g. [28].

Acknowledgments

We thank M. Fagerburg for supplying the photographs in Fig. 3, Dr. M. Tomschik for preparing the nucleosomes used in Fig. 8, and Dr. R. Steinman for critical reading. Supported by NIH K22CA077871, RO1GM077872 and startup funds from the University of Pittsburgh School of Medicine. L.S.G. acknowledges the support of the NIST Physics Laboratory and the NIST Director's Competence Program.

Certain commercial equipment, instruments, or materials are identified in this paper to foster understanding. Such identification does not imply recommendation or endorsement by the National Institute of Standards and Technology, nor does it imply that the materials or equipment identified are necessarily the best available for the purpose.

References

- [1] T. Basche, W.E. Moerner, M. Orrit, U.P. Wild (Eds.), *Single-Molecule Optical Detection, Imaging and Spectroscopy*, VCH Verlagsgesellschaft mbH, Weinheim, 1996.
- [2] March issue devoted to reviews on single-molecule approaches, *Science* 283 (1999).
- [3] K. van Holde, Minireview series on single-molecules, *J. Biol. Chem.* 274 (1999).

- [4] S.H. Leuba, J. Zlatanova (Eds.), *Biology At The Single-Molecule Level*, Pergamon, Amsterdam, 2001.
- [5] C. Zander, J. Enderlein, R.A. Keller (Eds.), *Single Molecule Detection In Solution*, Wiley-VCH, Berlin, 2002.
- [6] R. Rigler, T. Basche, M. Orrit (Eds.), *Single Molecule Spectroscopy: Nobel Conference Lectures*, Springer Verlag, Berlin, 2002.
- [7] S.H. Leuba, J. Zlatanova, *Arch. Histol. Cytol.* 65 (2002) 391–403.
- [8] J. Zlatanova, S.H. Leuba, *J. Muscle Res. Cell Motil.* 23 (2002) 377–395.
- [9] J. Zlatanova, *J. Biol. Chem.* 278 (2003) 23213–23216.
- [10] J. Zlatanova, S.H. Leuba, *Biochem. Cell Biol.* 81 (2003) 151–159.
- [11] J. Zlatanova, S.H. Leuba, *J. Mol. Biol.* 331 (2003) 1–19.
- [12] J. Zlatanova, S.H. Leuba, in: J. Zlatanova, S.H. Leuba (Eds.), *Chromatin Structure and Dynamics: State-of-the-Art*, Vol. 39, Elsevier, Amsterdam, 2004, pp. 369–396.
- [13] S.H. Leuba, M.L. Bennink, J. Zlatanova, in: C. Wu, C.D. Allis (Eds.), *Methods Enzymol.* 376 (2004) 73–105.
- [14] M.L. Bennink, S.H. Leuba, J. Zlatanova, in: E. Golemis, P. Adams (Eds.), *Protein–Protein Interactions, A Molecular Cloning Manual*, second ed., Cold Spring Harbor Laboratory Press, Cold Spring Harbor, 2005, pp. 415–427.
- [15] H.C. Zheng, M. Tomschik, J. Zlatanova, S.H. Leuba, in: E. Golemis, P. Adams (Eds.), *Protein-Protein Interactions, A Molecular Cloning Manual*, second ed., Cold Spring Harbor Laboratory Press, Cold Spring Harbor, 2005, pp. 429–444.
- [16] C. Claudet, J. Bednar, *Eur. Phys. J. E Soft Matter* 19 (2006) 331–337.
- [17] K. van Holde, J. Zlatanova, *J. Biol. Chem.* 281 (2006) 12197–12200.
- [18] M.L. Bennink, S.H. Leuba, G.H. Leno, J. Zlatanova, B.G. de Grooth, J. Greve, *Nat. Struct. Biol.* 8 (2001) 606–610.
- [19] B.D. Brower-Toland, C.L. Smith, R.C. Yeh, J.T. Lis, C.L. Peterson, M.D. Wang, *Proc. Natl. Acad. Sci. USA* 99 (2002) 1960–1965.
- [20] B. Brower-Toland, D.A. Wacker, R.M. Fulbright, J.T. Lis, W.L. Kraus, M.D. Wang, *J. Mol. Biol.* 346 (2005) 135–146.
- [21] C. Claudet, D. Angelov, P. Bouvet, S. Dimitrov, J. Bednar, *J. Biol. Chem.* 280 (2005) 19958–19965.
- [22] L.H. Pope, M.L. Bennink, K.A. van Leijenhurst-Groener, D. Nikova, J. Greve, J.F. Marko, *Biophys. J.* 88 (2005) 3572–3583.
- [23] G.J. Gemmen, R. Sim, K.A. Haushalter, P.C. Ke, J.T. Kadonaga, D.E. Smith, *J. Mol. Biol.* 351 (2005) 89–99.
- [24] A. Bancaud, N. Conde e Silva, M. Barbi, G. Wagner, J.F. Allemand, J. Mozziconacci, C. Lavelle, V. Croquette, J.M. Victor, A. Prunell, J.L. Viovy, *Nat. Struct. Mol. Biol.* 13 (2006) 444–450.
- [25] B. Ladoux, J.P. Quivy, P. Doyle, O. du Roure, G. Almouzni, J.L. Viovy, *Proc. Natl. Acad. Sci. USA* 97 (2000) 14251–14256.
- [26] M.L. Bennink, L.H. Pope, S.H. Leuba, B.G. de Grooth, J. Greve, *Single Mol.* 2 (2001) 91–97.
- [27] S.H. Leuba, M.A. Karymov, M. Tomschik, R. Ramjit, P. Smith, J. Zlatanova, *Proc. Natl. Acad. Sci. USA* 100 (2003) 495–500.
- [28] M. Tomschik, H.C. Zheng, K. van Holde, J. Zlatanova, S.H. Leuba, *Proc. Natl. Acad. Sci. USA* 102 (2005) 3278–3283.
- [29] T. Ha, A.Y. Ting, J. Liang, W.B. Caldwell, A.A. Deniz, D.S. Chemla, P.G. Schultz, S. Weiss, *Proc. Natl. Acad. Sci. USA* 96 (1999) 893–898.
- [30] X. Zhuang, L.E. Bartley, H.P. Babcock, R. Russell, T. Ha, D. Herschlag, S. Chu, *Science* 288 (2000) 2048–2051.
- [31] H.D. Kim, G.U. Nienhaus, T. Ha, J.W. Orr, J.R. Williamson, S. Chu, *Proc. Natl. Acad. Sci. USA* 99 (2002) 4284–4289.
- [32] X. Zhuang, H. Kim, M.J. Pereira, H.P. Babcock, N.G. Walter, S. Chu, *Science* 296 (2002) 1473–1476.
- [33] E. Tan, T.J. Wilson, M.K. Nahas, R.M. Clegg, D.M. Lilley, T. Ha, *Proc. Natl. Acad. Sci. USA* 100 (2003) 9308–9313.
- [34] L.E. Bartley, X. Zhuang, R. Das, S. Chu, D. Herschlag, *J. Mol. Biol.* 328 (2003) 1011–1026.
- [35] M.K. Nahas, T.J. Wilson, S. Hohng, K. Jarvie, D.M. Lilley, T. Ha, *Nat. Struct. Mol. Biol.* 11 (2004) 1107–1113.
- [36] S.A. McKinney, A.C. Declais, D.M. Lilley, T. Ha, *Nat. Struct. Biol.* 10 (2003) 93–97.
- [37] S.A. McKinney, E. Tan, T.J. Wilson, M.K. Nahas, A.C. Declais, R.M. Clegg, D.M. Lilley, T. Ha, *Biochem. Soc. Trans.* 32 (2004) 41–45.
- [38] M. Karymov, D. Daniel, O.F. Sankey, Y.L. Lyubchenko, *Proc. Natl. Acad. Sci. USA* 102 (2005) 8186–8191.
- [39] S.A. McKinney, A.D. Freeman, D.M. Lilley, T. Ha, *Proc. Natl. Acad. Sci. USA* 102 (2005) 5715–5720.
- [40] J.Y. Lee, B. Okumus, D.S. Kim, T. Ha, *Proc. Natl. Acad. Sci. USA* 102 (2005) 18938–18943.
- [41] C. Buranachai, S.A. McKinney, T. Ha, *Nano. Lett.* 6 (2006) 496–500.
- [42] T. Ha, I. Rasnik, W. Cheng, H.P. Babcock, G.H. Gauss, T.M. Lohman, S. Chu, *Nature* 419 (2002) 638–641.
- [43] I. Rasnik, S. Myong, W. Cheng, T.M. Lohman, T. Ha, *J. Mol. Biol.* 336 (2004) 395–408.
- [44] S. Myong, I. Rasnik, C. Joo, T.M. Lohman, T. Ha, *Nature* 437 (2005) 1321–1325.
- [45] C. Joo, S.A. McKinney, M. Nakamura, I. Rasnik, S. Myong, T. Ha, *Cell* 126 (2006) 515–527.
- [46] T. Forster, *Naturwissenschaften* 33 (1946) 166–175.
- [47] L. Stryer, R.P. Haugland, *Proc. Natl. Acad. Sci. USA* 58 (1967) 719–726.
- [48] R.M. Clegg, *Methods Enzymol.* 211 (1992) 353–388.
- [49] T. Ha, *Methods* 25 (2001) 78–86.
- [50] A.A. Deniz, M. Dahan, J.R. Grunwell, T. Ha, A.E. Faulhaber, D.S. Chemla, S. Weiss, P.G. Schultz, *Proc. Natl. Acad. Sci. USA* 96 (1999) 3670–3675.
- [51] A.A. Deniz, T.A. Laurence, G.S. Beligere, M. Dahan, A.B. Martin, D.S. Chemla, P.E. Dawson, P.G. Schultz, S. Weiss, *Proc. Natl. Acad. Sci. USA* 97 (2000) 5179–5184.
- [52] D.S. Talaga, W.L. Lau, H. Roder, J. Tang, Y. Jia, W.F. DeGrado, R.M. Hochstrasser, *Proc. Natl. Acad. Sci. USA* 97 (2000) 13021–13026.
- [53] B. Schuler, E.A. Lipman, W.A. Eaton, *Nature* 419 (2002) 743–747.
- [54] P.J. Rothwell, S. Berger, O. Kensch, S. Felekyan, M. Antonik, B.M. Wohrl, T. Restle, R.S. Goody, C.A. Seidel, *Proc. Natl. Acad. Sci. USA* 100 (2003) 1655–1660.
- [55] E.A. Lipman, B. Schuler, O. Bakajin, W.A. Eaton, *Science* 301 (2003) 1233–1235.
- [56] B. Schuler, E.A. Lipman, P.J. Steinbach, M. Kumke, W.A. Eaton, *Proc. Natl. Acad. Sci. USA* 102 (2005) 2754–2759.
- [57] P. Zhu, J.P. Clamme, A.A. Deniz, *Biophys. J.* 89 (2005) L37–L39.
- [58] J.P. Clamme, A.A. Deniz, *Chemphyschem.* 6 (2005) 74–77.
- [59] E. Boukobza, A. Sonnenfeld, G. Haran, *J. Phys. Chem. B* 105 (2001) 12165–12170.
- [60] E. Rhoades, E. Gussakovsky, G. Haran, *Proc. Natl. Acad. Sci. USA* 100 (2003) 3197–3202.
- [61] B. Okumus, T.J. Wilson, D.M. Lilley, T. Ha, *Biophys. J.* 87 (2004) 2798–2806.
- [62] J.E. Reiner, A.M. Crawford, R.B. Kishore, L.S. Goldner, K. Helmerston, M.K. Gilson, *Appl. Phys. Lett.* 89 (2006) 013904.
- [63] E.B. Shera, N.K. Seitzinger, L.M. Davis, R.A. Keller, S.A. Soper, *Chem. Phys. Lett.* 174 (1990) 553–557.
- [64] S.A. Soper, E.B. Shera, J.C. Martin, J.H. Jett, J.H. Hahn, H.L. Nutter, R.A. Keller, *Anal. Chem.* 63 (1991) 432–437.
- [65] E. Betzig, R.J. Chichester, *Science* 262 (1993) 1422–1425.
- [66] X.S. Xie, R.C. Dunn, *Science* 265 (1994) 361–364.
- [67] W.P. Ambrose, P.M. Goodwin, J.C. Martin, R.A. Keller, *Phys. Rev. Lett.* 72 (1994) 160–163.
- [68] D. Axelrod, *Methods Cell Biol.* 30 (1989) 245–270.
- [69] T. Funatsu, Y. Harada, M. Tokunaga, K. Saito, T. Yanagida, *Nature* 374 (1995) 555–559.
- [70] M. Ishikawa, K. Hirano, T. Hayakawa, S. Hosoi, S. Brenner, *Jap. J. Appl. Phys.* 33 (1994) 1571–1576.
- [71] I. Sase, H. Miyata, J.E.T. Corrie, J.S. Craik, K. Kinosita Jr., *Biophys. J.* 69 (1995) 323–328.
- [72] T. Schmidt, G.J. Schutz, W. Baumgartner, H.J. Gruber, H. Schindler, *J. Phys. Chem.* 99 (1995) 17662–17668.
- [73] T. Schmidt, G.J. Schutz, W. Baumgartner, H.J. Gruber, H. Schindler, *Proc. Natl. Acad. Sci. USA* 93 (1996) 2926–2929.
- [74] M. Orrit, J. Bernard, *Phys. Rev. Lett.* 65 (1990) 2716–2719.
- [75] W.P. Ambrose, T. Basche, W.E. Moerner, *J. Chem. Phys.* 95 (1991) 7150–7163.

- [76] W.P. Ambrose, W.E. Moerner, *Nature* 349 (1991) 225–227.
- [77] T. Basche, W.E. Moerner, M. Orrit, H. Talon, *Phys. Rev. Lett.* 69 (1992) 1516–1519.
- [78] M. Minsky, U.S. Patent Office, vol. 10, U.S. 3,013,467, 1961.
- [79] S. Nie, D.T. Chiu, R.N. Zare, *Science* 266 (1994) 1018–1021.
- [80] U. Mets, R. Rigler, *J. Fluorescence* 4 (1994) 259–264.
- [81] J.J. Macklin, J.K. Trautman, T.D. Harris, L.E. Brus, *Science* 272 (1996) 255–258.
- [82] J. Dapprich, U. Mets, W. Simm, M. Eigen, R. Rigler, *Exp. Tech. Phys.* 41 (1995) 259–264.
- [83] T. Ha, T. Enderle, D.F. Ogletree, D.S. Chemla, P.R. Selvin, S. Weiss, *Proc. Natl. Acad. Sci. USA* 93 (1996) 6264–6268.
- [84] P.R. Selvin, *Nat. Struct. Biol.* 7 (2000) 730–734.
- [85] W.E. Moerner, D.P. Fromm, *Ref. Sci. Instr.* 74 (2003) 3597–3619.
- [86] X. Michalet, A.N. Kapanidis, T. Laurence, F. Pinaud, S. Doose, M. Pflughoefft, S. Weiss, *Annu. Rev. Biophys. Biomol. Struct.* 32 (2003) 161–182.
- [87] S. Weiss, *Science* 283 (1999) 1676–1683.
- [88] T. Plakhotnik, E.A. Donley, U.P. Wild, *Annu. Rev. Phys. Chem.* 48 (1997) 181–212.
- [89] R.A. Keller, W.P. Ambrose, P.M. Goodwin, J.H. Jett, J.C. Martin, M. Wu, *Appl. Spectrosc.* 50 (1996) 12A–32A.
- [90] W. Min, B.P. English, G. Luo, B.J. Cherayil, S.C. Kou, X.S. Xie, *Acc. Chem. Res.* 38 (2005) 923–931.
- [91] A. Ishijima, T. Yanagida, *Trends Biochem. Sci.* 26 (2001) 438–444.
- [92] A.A. Deniz, T.A. Laurence, M. Dahan, D.S. Chemla, P.G. Schultz, S. Weiss, *Annu. Rev. Phys. Chem.* 52 (2001) 233–253.
- [93] S. Weiss, *Nat. Struct. Biol.* 7 (2000) 724–729.
- [94] X.S. Xie, H.P. Lu, *J. Biol. Chem.* 274 (1999) 15967–15970.
- [95] X. Michalet, S. Weiss, M. Jager, *Chem. Rev.* 106 (2006) 1785–1813.
- [96] R.B. Mujumdar, L.A. Ernst, S.R. Mujumdar, C.J. Lewis, A.S. Waggoner, *Bioconjug. Chem.* 4 (1993) 105–111.
- [97] A.N. Kapanidis, N.K. Lee, T.A. Laurence, S. Doose, E. Margeat, S. Weiss, *Proc. Natl. Acad. Sci. USA* 101 (2004) 8936–8941.
- [98] N.K. Lee, A.N. Kapanidis, Y. Wang, X. Michalet, J. Mukhopadhyay, R.H. Ebricht, S. Weiss, *Biophys. J.* 88 (2005) 2939–2953.
- [99] C.R. Sabanayagam, J.S. Eid, A. Meller, *J. Chem. Phys.* 123 (2005) 224708.
- [100] R. Holliday, *Genet. Res. Camb.* 5 (1964) 282–304.
- [101] M. Tomschik, M.A. Karymov, J. Zlatanova, S.H. Leuba, *Structure* 9 (2001) 1201–1211.
- [102] K.T. Fry, R.A. Lazzarini, San A. Pietro, *Proc. Natl. Acad. Sci. USA* 50 (1963) 652–657.
- [103] Y. Harada, K. Sakurada, T. Aoki, D.D. Thomas, T. Yanagida, *J. Mol. Biol.* 216 (1990) 49–68.
- [104] I. Rasnik, S.A. McKinney, T. Ha, *Nat. Methods* 3 (2006) 891–893.
- [105] T. Förster, *Discuss. Faraday Soc.* 27 (1959) 7–17.
- [106] W.L. DeLano, *The PyMOL Molecular Graphics System*, DeLano Scientific, San Carlos, 2002.
- [107] D.E. McRee, *Practical protein crystallography*, Academic Press, San Diego, 1993.
- [108] C.A. Davey, D.F. Sargent, K. Luger, A.W. Maeder, T.J. Richmond, *J. Mol. Biol.* 319 (2002) 1097–1113.